# PROBING HADRON PROPERTIES WITH SCATTERING

MARKO MALEŽIČ

Fakulteta za matematiko in fiziko
Univerza v Ljubljani

An important study in quantum mechanics is the study of scattering. By employing scattering, it is possible to find new states that can be bound or short-lived. In this paper, We will formally derive the scattering amplitude for scattering on the potential and express it with a phase shift. Although this approach is quite restrictive, it still produces important results. It renders information on the interaction between particles and reveals properties of bound states and resonances. After the theoretical formalism, We will give some examples of states studied numerically and experimentally. Although scattering is present in many fields of physics, We will focus on examples from hadron particle physics.

**RAZKRIVANJE HADRONSKIH LASTNOSTI PREKO SIPANJA**

Pomemben del kvantne mehanike je raziskava sipanja. Preko uporabe sipanja kot orodja, je možno najti nova stanja, ki so lahko vezana ali kratkoživa. V tem članku, bomo formalno izpeljali sipalno amplitudo za sipanje na potencialni jami in jo zapisali preko faznega zamika. Čeprav je pristop omejevalen, prinese s seboj nekaj pomembnih rezultatov. Razkrije informacijo o interakciji med delci in prikaže lastnosti vezanih stanj ter resonanc. Po teoretičnem formalizmu bomo podali nekaj primerov stanj, ki jih lahko študiramo numerično in eksperimentalno. Čeprav je sipanje prisotno v skoraj vseh območjih fizike, se bomo osredotočili na primere iz hadronske fizike delcev.

## 1. Introduction

Scattering is a valuable tool in physics. It is present in many areas of physics, like optics, solid state, and particle physics. Since scattering is a process of interaction between a particle and some medium, it depends on the types of particles and mediums. In optics, the particle is light, and its medium is the lens. The particle might be a phonon in solid-state physics, and the medium is the crystalline lattice. Finally, in particle physics, the medium is also a particle, and the scattering of two particles can produce new states.

The research on scattering in quantum mechanics starts with the time-dependent Schrödinger equation. There are many approaches to solving it. A simple way is to expand the particle wave into a spherical wave far away from the scattering center. The only difference between the spherical incoming and outgoing waves is the phase shift $\delta$, which contains the interaction information. From this, we can calculate the scattering amplitude and find the relation between the phase shift $\delta$ and the scattering matrix S. This approach to scattering has been very useful in particle physics. It has contributed to our understanding of hadrons and their interactions.

The scattering amplitude renders valuable information on the properties of states. We will argue that states are related to the poles of the scattering amplitude that is expressed in terms of energy. We have to define a boundary in the spectrum, the threshold. Consider the scattering of two non-relativistic particles with masses $m_1$ and $m_2$. The system's energy is defined by the masses of the particles: $W = (m_1 + m_2)c^2 + E$, where $E$ is the kinetic and potential energy. The threshold is then defined as $E = 0$. If the pole energy is below the threshold ($E \leq 0$), the state is bound and it doesn't decay. Examples of bound states would be the proton or deuterium (bound proton and neutron). However, if the pole energy is above the threshold ($E \geq 0$), the new state is called a resonance, and it decays. There are many resonances in particle physics, and more are being discovered. Currently, exciting new hadronic states are called exotic and are believed to be made from four (tetraquark) or five valence quarks (pentaquark). These states can be studied either experimentally (through particle colliders and detectors) or numerically (through the discretization of space-time).

## 2. Scattering formalism

To understand the experimental and numerical results, let us first establish a formal understanding of scattering. Consider the scattering of a plane wave on a finite potential. Our approach will be to start with the spherical wave expansion of the particle wave, from which we'll derive the scattering amplitude. This will be convenient for the investigation of bound and unbound states ([1], [2]).

Before we start, let us assume the interaction potential has a finite range (Figure 2), which lets us expand the wave far from the interaction. In the formalism, elastic scattering is also assumed, which means that the probability flux is conserved. We should note that with all of these assumptions, this approach falls short in correct studies of more complex processes. However, it is a good representation of scattering and gives a few important results.

In the first step, initial and final states are expanded into spherical waves using the Legendre polynomials $P_l$ (Figure 1). Far from the scattering center, the final state must be described by an outgoing spherical wave. The conservation of probability implies that the absolute values of pre-factors for ingoing and outgoing waves must be equal. They can only differ by the phase factor, which is denoted by $S_l = \exp(2i\delta_l)$. Since this is the only difference, it must contain information about the interaction,

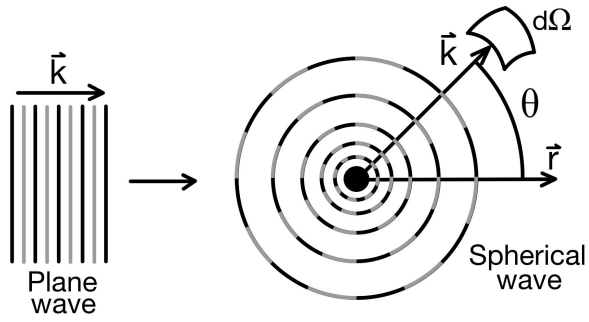


**Figure 1.** Spherical wave expansion. The wave vector $\vec{k}$ is pointing to a differential solid angle dΩ.

$$\psi_i = \frac{1}{\sqrt{V}} e^{ikz} = \frac{1}{\sqrt{V}} \frac{i}{2kr} \sum_l (2l+1) \left[ (-1)^l e^{-ikr} - e^{ikr} \right] P_l(\cos\theta), \tag{1}$$

$$\psi_f = \frac{1}{\sqrt{V}} \frac{i}{2kr} \sum_l (2l+1) \left[ (-1)^l e^{-ikr} - S_l e^{ikr} \right] P_l(\cos\theta), \tag{2}$$

We've introduced the phase shift $\delta_l$. Since it will be useful in studying bound states, let us look at how it impacts the wave function. Far from the scattering center ($kr \gg 1$) and outside a general potential, the equation (2) has the following asymptotic expansion (3)[1],

$$\psi(r) \sim \frac{1}{r} \sin(kr + \delta_l). \tag{3}$$

With our focus being on scattering, it is better to write the final state as a sum of the initial plane wave (1) and a scattered spherical wave. This form lets us continue the formalism through the use of the scattering amplitude $A(\theta)$,

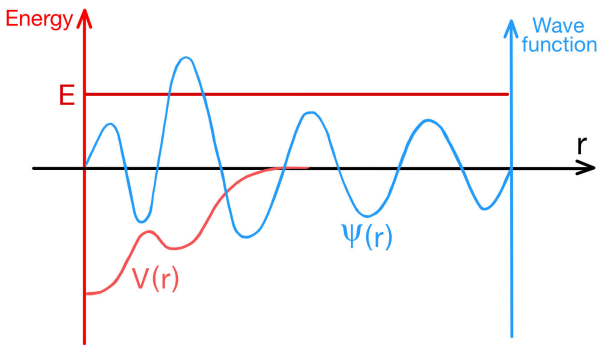


**Figure 2.** Sketch of the solution $\psi(r)$ inside and outside the potential $V(r)$.

$$\psi_f = \frac{1}{\sqrt{V}} \left( e^{ikz} + A(\theta) e^{ikr}/r \right), \quad A(\theta) = \frac{1}{k} \sum_l (2l+1) f_l P_l(\cos\theta). \tag{4}$$

[1] In general, the function has the form of Bessel functions.

The amplitude $A$ contains the term $f_l$, which can be found by comparing the final state $\psi_f$ in both forms (2, 4). The form (5) is useful for further analysis of the scattering,

$$f_l = \frac{e^{2i\delta_l} - 1}{2i}. \tag{5}$$

Let us now determine the relation between the scattering amplitude and the cross section, which is an observable quantity, for spinless particles. On the one hand, we know the flux of scattered particles $\Phi_f$ can be calculated from the probability the scattered particle passes through the differential solid angle $\mathrm{d}\Omega$ (Figure 1),

$$\mathrm{d}\Phi_f = \rho_f v \mathrm{d}S = \frac{1}{V} v |A(\theta)|^2 \mathrm{d}\Omega, \tag{6}$$

where $\rho_f = |\psi_{out}|^2 = |A(\theta)|^2/r^2$ is the probability density of the outgoing wave term in (4), $v$ the velocity of the particle, and $\mathrm{d}S = r^2 \mathrm{d}\Omega$. On the other hand, the same flux is proportional to the cross section $\sigma$, which is observable, $\Phi_f = j_i \sigma(i \to f)$, where $j_i = v/V$ is the flux of incoming particles. Combining this equation with (6), a relation between the differential cross section and the scattering amplitude can be found[2],

$$\frac{\mathrm{d}\sigma}{\mathrm{d}\Omega} = |A(\theta)|^2. \tag{7}$$

To get the total cross section, the differential cross section has to be integrated (7) over the solid angle $\Omega$. The only dependence on $\Omega$ is present in the Legendre polynomials $P_l(\cos\theta)$. By employing the orthogonality of $P_l$ the integral is found to be, $\int P_l(\cos\theta) P_{l'}(\cos\theta) \mathrm{d}\Omega = 4\pi\delta_{ll'}/(2l+1)$. Using this result, we calculate the final result for the cross section as

$$\sigma = \frac{4\pi}{k^2} \sum_l (2l+1) \left| \frac{e^{2i\delta_l} - 1}{2i} \right|^2 = \frac{4\pi}{k^2} \sum_l (2l+1) \sin^2 \delta_l. \tag{8}$$

## 3. Scattering on a potential well

We will examine a case of scattering on a potential well in three dimensions, which is a useful approximation for specific types of interactions. Its study leads to a better understanding of the nuclear force [5].

Since we will restrict ourselves to scattering at low energies, it is enough to expand our states using only $l = 0$. With this assumption, the solution can be easily found inside and outside the potential by using (2, 3). Another way would be to solve the Schrödinger equation,

$$u(r) = \begin{cases} A \sin qr, & r \le R \\ B \sin(kr + \delta_0), & r \ge R \end{cases}, \tag{9}$$
$$q^2 = 2m_r(E + V_0),$$
$$k^2 = 2m_r E.$$

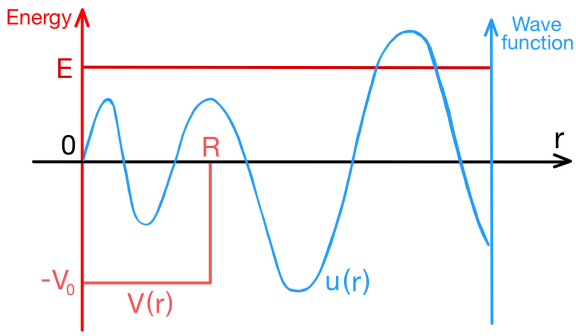


**Figure 3.** Sketch of the solution (9) with a representation of the potential $V(r)$ and positive energy $E$.

[2] A better understanding of the formalism behind cross section is given in [4].

Since $u(r)$ in eq. (9) has to be continuous and continuously derivative at $r = R$, we can derive the phase shift for a finite potential well. Dividing equations $u(R) = A \sin qR = B \sin(kR + \delta_0)$ and $u'(R) = qA \cos qR = kB \cos(kR + \delta_0)$, results in an expression for $\delta_0$

$$\delta_0 = \arctan\left(\frac{k}{q} \tan qR\right) - kR + n\pi, \quad n \in Z. \tag{10}$$

From the equation (10) it is clear to see the interaction information in $\delta_0$, since its parameters are the well depth $V_0$ (inside $q$) and width $R$.

With a formal expression for the phase shift, the cross section can now be calculated, since that's what is measured in the experiment. The first step is to calculate $\sin \delta_0$ from the cross section expansion (8). In the low energy range, both the tangent and the sine functions can be expanded using a Taylor series, $\sin x = \arctan x = x + \mathcal{O}(x^3)$, which leaves us with the following form,

$$\sin \delta_0 = k\left(\frac{1}{q} \tan qR - R\right) = ka, \tag{11}$$

$$a = \frac{1}{q} \tan qR - R, \tag{12}$$

where the scattering length $a$ was introduced, which is used in the low-energy region. The scattering length is also related to the geometrical cross-section. Inserting this result (11, 12) into the cross section (8) the relation between it and the scattering length $a$ is found to be

$$\sigma = 4\pi a^2. \tag{13}$$

## 4. Proton-neutron scattering and deuterium

Let us use the knowledge gained from the phase shift formalism as an example. We would like to explore the properties of deuterium, a bound state containing one proton and one neutron, by scattering protons and neutrons (a representation is shown in Figure 4). To determine deuterium's potential properties ($V_0$, $R$), experimental data on its binding energy $E_v$ and the cross section $\sigma$ is needed.

Deuterium is a similar system to the one discussed in the previous section. The only difference being that the energy is negative ($E \leq 0$). The solution to this Schrödinger equation is also similar, except that the function outside the well exponentially falls to zero [5]. In this system, we need to be careful with the momenta $k$ and $q$. The momentum outside the well $k$ is imaginary, which is the cause of the exponential. Using the same boundary conditions as we did with scattering, the second relation needed to calculate the potential is found to be,

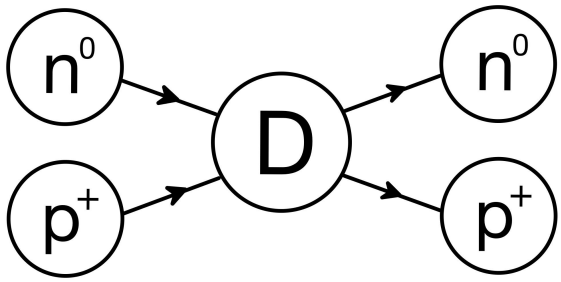


**Figure 4.** The scattering of a proton and a neutron produces deuterium, which decays back into the original nucleons.

$$\frac{1}{q} \tan qR = -\frac{1}{|k|}; \quad k = i\sqrt{2m|E|}, \quad q = \sqrt{2m(V_0 - E)}. \tag{14}$$

The complex momenta also lead to the scattering amplitude having poles in the negative region. Applying $k$ to the equation (4) poles are found at the bound state mass, $S(m_b) = \infty$.

We have to take into account the fact that nucleons have spin, which affects the potential. Each nucleon has spin $J = 1/2$, making their new state deuterium either a singlet (spin $J = 0$) or a triplet (spin $J = 1$). It turns out that the bound state is the triplet, while the singlet doesn't form a bound state because its potential is weaker. The addition of spins also leads to separate cross sections. The average cross section is then the sum of both parts weighted by the probability of measuring one state or the other (15),

$$\overline{\sigma} = \frac{1}{4}\sigma_s + \frac{3}{4}\sigma_t. \tag{15}$$

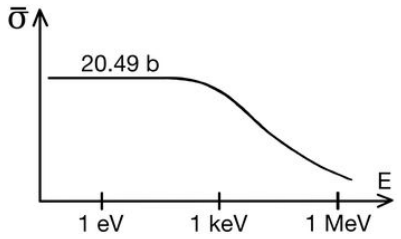


**Figure 5.** Proton-neutron scattering cross section's dependency of energy. $\sigma$ is almost constant for low energy but starts decreasing around $E = 200$ eV. The figure was constructed with data from [6]

The triplet is three times as likely to be measured since there are three possible projections of spin ($J_3 = -1, 0, 1$), while the singlet only has one ($J_3 = 0$). The energy dependence of the average cross section for proton-neutron scattering is shown in Figure 5.

With the experimental results for separate cross sections ($\sigma_s$, $\sigma_t$) and the binding energy $E_b$, we now have everything we need to describe deuterium's potential. The well depth needs to be determined for the singlet ($V_s$) and triplet ($V_t$) and assuming they both have the same width $R$, the full potential can be calculated. We have to stress that the calculation works for low scattering energies and for this simple form of the potential. First, the binding energy has to be measured $E_b = -2.2$ MeV and an experiment scattering polarized particles measures different cross sections, which leads us to calculate the scattering lengths $a_s$ and $a_t$ by use of (13). Finally, combining equations (12) for different spins and (14) leads us to calculate $V_s$, $V_t$ and $R$ [5]. Results are shown in Table 1.

| J | $\sigma$ [b] | a [fm] | V [MeV] | R [fm] |
|---|---|---|---|---|
| 0 | 67 | 23.67 | 23.4 | 2.02 |
| 1 | 5 | -5.40 | 36.2 | 2.02 |

**Table 1.** Experimental results for deuterium with different spins $J$. $\sigma$ - cross section, $a$ - scattering length, $V$ - potential depth, $R$ - potential width

Since bound states have negative energy, they can't be produced through scattering. Nonetheless, scattering still provides enough information to construct a good understanding of the bound state, as shown in the example. It is interesting to study bound states theoretically, where negative energy is technically allowed.

## 5. Resonances - $\rho$ meson

We used the scattering formalism to explore bound states. Let us now focus on the spectrum above the threshold energy, where additional poles can be found in the scattering amplitude. These poles correspond to metastable particles, which can be observed. They are responsible for peaks in the cross section. Determining the extremes of the cross section (8) leads to the phase shift condition $\delta_l^R = \delta_l(E_R) = \pi/2$. This is called a resonance, and $E_R$ is therefore the resonance energy. Our goal is to understand the dependence of the cross section on the energy around the maximum. It is convenient to express $f_l$ (5) in terms of $\cot\delta_l$ and expand it with a Taylor series [3],

$$f_l = \frac{i}{1 - e^{2i\delta_l}} = \frac{1}{\cot\delta_l - i},$$
$$\cot\delta_l \approx \cot\delta_l(E_R) + (E - E_R)\left[\frac{\mathrm{d}}{\mathrm{d}E}\cot\delta_l(E)\right]_{E=E_R}. \tag{16}$$

The first term in (16) vanishes since $\delta_l(E_R) = \pi/2$ and resonance width $\Gamma$ is introduced. Using the new parametrization, we can express $\delta_l$ (shown in the upper graph in Figure 6) and $f_l$ as

$$\cot \delta_l \approx -\frac{2(E - E_R)}{\Gamma}, \quad \Gamma/2 = -\left[\frac{\mathrm{d}}{\mathrm{d}E} \cot \delta_l(E)\right]_{E=E_R}, \tag{17}$$

$$f_l \approx \frac{\Gamma/2}{(E - E_R) - i\Gamma/2} \tag{18}$$

The parameter $\Gamma$ can be interpreted as the width of the distribution, similar to the standard deviation of the Gaussian function. Since the intermediate state is unstable, the resonance width can be related to the decay time through the Planck constant, $\tau = \hbar/\Gamma$. Expressing the cross section (7) with the approximation for $f_l$ (18), we find the expression for the Breit-Wigner resonance curve. It describes the behavior of the cross section around the resonance energy (shown in the lower graph in Figure 6). Since the resonance has a defined spin and parity, only one partial wave $l$ dominates near resonance energy,

$$\sigma^l \approx \frac{4\pi}{k^2}(2l + 1)\frac{\Gamma^2/4}{(E - E_R)^2 + \Gamma^2/4} \tag{19}$$

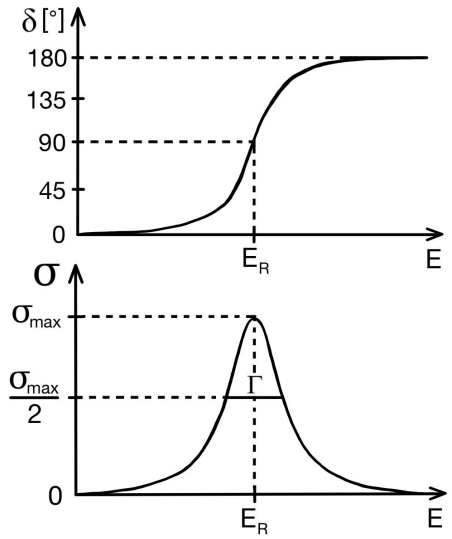


**Figure 6.** Breit-Wigner resonance curves for the phase shift (17) (above) and the cross section (19) (below).

After acquiring the necessary knowledge to study resonances, let us now look at an example. We'll analyze one of the simplest resonances, the meson $\rho(770)$. This resonance is one of the easiest to investigate theoretically since it is far away from the inelastic region, where our formulation of scattering becomes less reliable. Furthermore, only the p-wave ($l = 1$) is used in the series, since both pions ($\pi$) have spin $J = 0$, while $\rho$ has spin $J = 1$. A similar but more difficult study would be the $f_0(500)$ (also known as $\sigma$) and a strange $\mathrm{K}^*(892)$ resonance.

The $\rho$ meson decays almost exclusively into two pions $\pi$, implying that it can be created through the scattering of two pions as well. A representation of such a scattering at the quark level is shown in Figure 7[3]. Two experimental results are shown in Figure 8 and present a clear Breit-Wigner resonance curve for phase shifts (17) and the cross section (19). Fitting the curves to the data resulted in the parameters for $\rho$. Both experiments found a similar result,

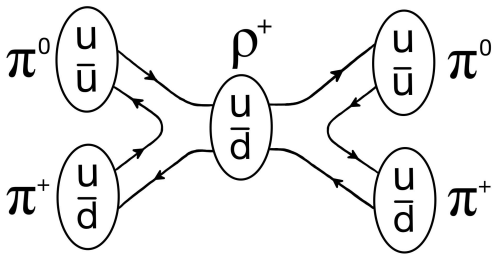


**Figure 7.** $\rho$ resonance through the scattering of two pions $\pi$.

$$M_\rho^\delta = 775 \pm 4\,\mathrm{MeV}, \qquad \Gamma_\rho^\delta = 160 \pm 10\,\mathrm{MeV},$$
$$M_\rho^\sigma = 775.1 \pm 0.7\,\mathrm{MeV}, \qquad \Gamma_\rho^\sigma = 147 \pm 1.5\,\mathrm{MeV}.$$

[3]Experimentally, however, it is easier to scatter more stable particles, which produce the $\rho$ resonance.

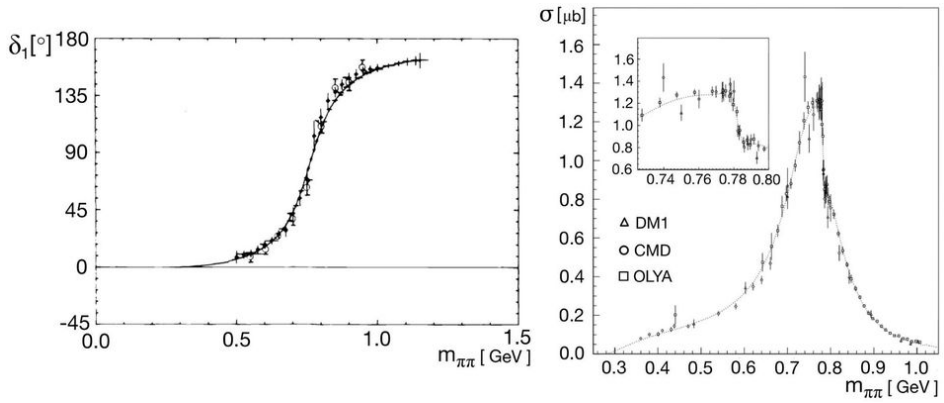


**Figure 8.** Experimental results in the study of the $\rho$ resonance. The dependence of phase shift for $l = 1$ (left) [7] and the cross section (right) [8] on energy. Both graphs show a characteristic Breit-Wigner resonance curve, similar to Figure 6.

Theoretically, we also have to study resonances through scattering, since they aren't stable. To achieve this, numerical methods are employed, which use quantum field theory on a lattice[4]. The approach is quite versatile, since the parameters of this method are the same as the parameters of the fundamental theory. This means we can compare numerical results with the experiment and study results with different parameters. This was done in the paper researching the $\rho$ resonance through quantum chromodynamics on the lattice, which is the only way to study the problem without perturbative expansion [9]. One of their results is the graph in Figure 9.
It shows the phase shift as a function of energy for different u and d quarks. The red line corresponds to the quark masses in Nature. Using the physically correct mass, the paper finds the numerical result corresponds with the experimental data,

$$M_\rho = 769 \pm 19\,\mathrm{MeV}$$
$$\Gamma_\rho = 129 \pm 7\,\mathrm{MeV}$$

As can be seen from Figure 9, the method allows for the study of non-physical parameters, which is useful when more complex particles are investigated.

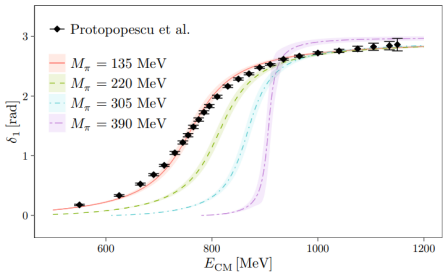


**Figure 9.** A theoretical study of $\rho$ resonance. The graph shows the Breit-Wigner resonance curves for the phase shift. Different colored lines represent different quark masses, where the red line represents the physical mass. Instead of quark masses, corresponding pion masses are presented ($m_q \propto m_\pi^2$) [9].

## 6. Exotic particles

So far, we discussed conventional hadrons, which consist of two or three valence quarks, using the $\rho$ meson as an example. However, a captivating and recent area of research in particle physics is focused on examining exotic hadrons. Exotic hadrons are made up of more than three constituent quarks (tetraquarks and pentaquarks) and maybe valence gluons (hybrid hadrons). The discovered particles are either resonances or shallow bound states. These have been discovered experimentally, but they are not yet fully understood theoretically.

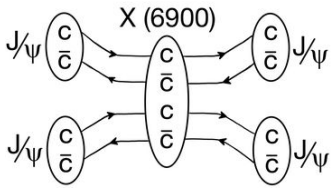


**Figure 10.** Scattering of two $J/\psi$, leads to an intermediate fully charming tetraquark $X(6900)$.

[4]The underlying fundamental theory of hadrons is quantum chromodynamics.

One such exotic particle is a tetraquark made up of four charm quarks ($c\bar{c}c\bar{c}$), called the fully charming tetraquark $X(6900)$. To form such a particle, one can scatter two particles made from two charm quarks ($c\bar{c}$), called $J/\psi$. This tetraquark was discovered at the LHCb experiment in 2020 at CERN[5]. The proton-proton collisions at the LHC gave rise to the $J/\psi$ scattering process sketched in Figure 10 as one of many possible intermediate processes. From the dataset, they counted the number of such processes as a function of the invariant di-$J/\psi$ mass[6] (refer to Figure 11). $X(6900)$ wasn't the only resonance discovered, but it was the easiest to determine. After fitting the Breit-Wigner curve, they found the following resonance parameters for $X(6900)$,

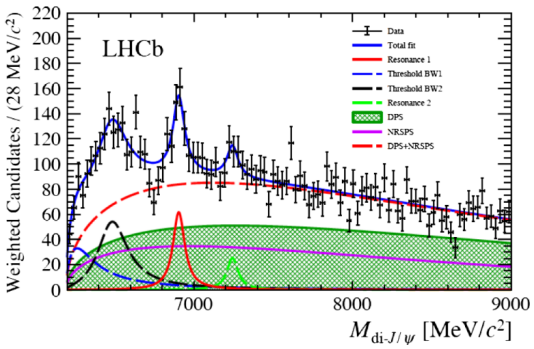


**Figure 11.** Candidates for the fully charming tetraquark as a function of the invariant di $J/\psi$ mass. Around 6900 MeV the collaboration found a peak, which corresponds to the X(6900) tetraquark resonance [10].

$$M[X(6900)] = 6905 \pm 11 \pm 7\,\text{MeV},$$
$$\Gamma[X(6900)] = 80 \pm 19 \pm 33\,\text{MeV}.$$

Another recently discovered exotic resonance is a pentaquark. In particular, the discovered pentaquark $P_c$ composed of u u d c $\bar{c}$ quarks, can be created by scattering protons and $J/\psi$ mesons as shown in Figure 12. The LHCb collaboration discovered it in 2015 and explored its properties [11]. A similar approach to analyzing the data was used as with the tetraquark. The data showed three peaks, corresponding to three different $P_c^+$ states (refer to Figure 13). Since two peaks were close together, fitting a mixture of Breit-Wigner curves was necessary to determine their mass and width. Results for $P_c^+$ properties are presented in Table 2.

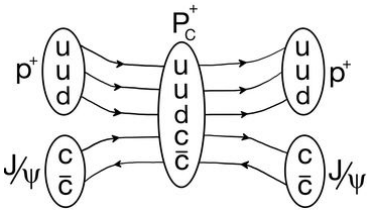


**Figure 12.** Scattering a proton $p+$ and a $J/\psi$ meson creates a resonance pentaquark $P_c^+$.

| State | M [MeV] | Γ [MeV] |
|---|---|---|
| $P_c^+(4312)$ | $4311.9 \pm 0.7^{+6.8}_{-0.6}$ | $9.8 \pm 2.7^{+3.7}_{-4.5}$ |
| $P_c^+(4440)$ | $4440.3 \pm 1.3^{+4.1}_{-4.7}$ | $20.6 \pm 4.9^{+8.7}_{-10.1}$ |
| $P_c^+(4457)$ | $4457.3 \pm 0.6^{+4.1}_{-1.7}$ | $6.4 \pm 2.0^{+5.7}_{-1.9}$ |

**Table 2.** Experimental results for different states of $P_c^+$ as seen in Figure 13. [11]

It is hard to study exotic particles theoretically because these two types of exotic particles have many decay channels. To correctly extract their properties theoretically, a much more complex formalism of inelastic scattering is needed.

In the last two decades, around 30 exotic hadrons have been discovered. Some of them have also been reliably studied and understood theoretically. As further research is conducted in this field, others are soon to follow.

[5]This discovery was later confirmed by the ATLAS and CMS collaborations.

[6]The invariant mass is an important quantity, when discussing inelastic scattering. It is the portion of the total mass of the system of objects that is independent of the overall motion of the system.

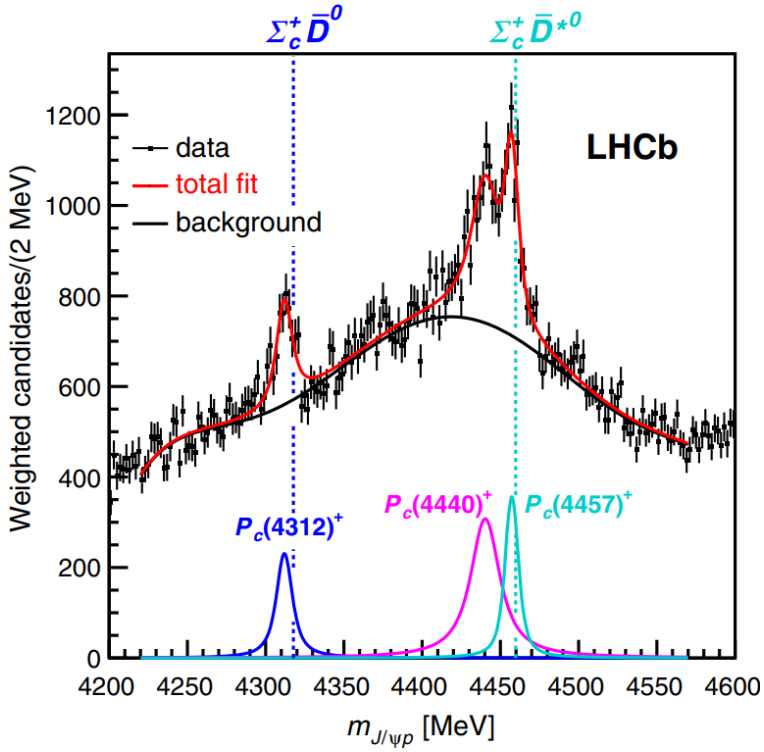


**Figure 13.** Candidate distribution as a function of $m_{pJ/\psi}$, with fits to three Breit-Wigner resonance curves. The fits determine the $P_c^+$ masses and widths [11].

## 7. Conclusions

Scattering is employed as a tool in many fields of physics, and its study leads to a better understanding of Nature. It is possible to solve scattering problems in quantum mechanics through the phase shift formalism. The formalism expresses results in terms of the phase shift, which is represented in the phase of the particle-wave far from the scattering center. Though a few assumptions need to be made, such an approach leads to important results. We focused on exploring these results in hadron physics. The first result was a qualitative description of bound states in relation to the properties of the binding potential. A simple but important example of this is the study of deuterium. The second result was a study of the scattering amplitude around the cross section maximum. This provides the Breit-Wigner resonance curve, which can be used to fit data. The fitted parameters correspond to mass and decay time. A simple example of a resonance is the $\rho$ meson. Recent research in experimental particle physics has discovered new exotic particles that differ from conventional hadrons in the number of valence quarks and gluons. This area of hadrons has not been fully explored experimentally and theoretically, but more research will soon lead to a better understanding of these particles.

## REFERENCES


[1] L. D. Landau and E. M. Lifshitz, *Quantum Mechanics* (Internet Archive, 1965), p. 469-472.

[2] J. E. Bowcock and H. Burkhardt, *Principles and problems of phase-shift analysis*, Rep. Prog. Phys. **38**, 1099 (1975), DOI: 10.1088/0034-4885/38/9/002.

[3] Jernej F. Kamenik and Boštjan Golob, *Rešene naloge iz fizike jedra in osnovnih delcev* (2011), p. 27-30 , `http://www-f1.ijs.si/~kosnik/fjod/` (2023).

[4] Micheal E. Peskin and Daniel V. Schroeder, *An Introduction to Quantum Field Theory* (Avalon Publishing, 1995), p. 99-108.

[5] Mitja Rosina, *Zbirka izbranih poglavij iz fizike 3., Jedrska fizika*, (DMFA, Ljubljana 2005), p. 54-64.

[6] W. Dilg, *Measurement of the neutron-proton total cross section at 132 eV*, Phys. Rev. C **11**, 103 (1975), DOI: `https://doi.org/10.1103/PhysRevC.11.103`.

[7] M. Benayoun, S. Eidelman, K. Maltman, H.B. O'Connell, B.Shwartz and A.G. Williams, *New results in $\rho^0$ meson physics*, Eur. Phys. J. C 2 (1998) p. 269-286, `https://arxiv.org/abs/hep-ph/9707509`.

[8] S. D. Protopopescu et al, *$\pi\pi$ Partial-Wave Analysis from Reactions $\pi+p \to \pi+\pi-\Delta^{++}$ and $\pi+p \to K+K-\Delta^{++}$ at 7.1 GeV/c*, Phys. Rev. D **7**, 1279 (1973), DOI: `https://doi.org/10.1103/PhysRevD.7.1279`.

[9] M. Werner, M. Ueding, C. Helmes et al., *Hadron–Hadron interactions from $N_f = 2 + 1 + 1$ lattice QCD: the $\rho$-resonance*, Eur. Phys. J. A **56**, 61 (2020), DOI: `https://doi.org/10.1140/epja/s10050-020-00057-4`.

[10] LHCb Collaboration, R. Aaij, et al., *Observation of structure in the $J/\psi$-pair mass spectrum*, Science Bulletin 65:1983–1993, DOI: `https://doi.org/10.1016/j.scib.2020.08.032`.

[11] LHCb Collaboration, R. Aaij, et al., *Observation of a Narrow Pentaquark State, $P_c(4312)^+$, and of the Two-Peak Structure of the $P_c(4450)^+$*, Phys. Rev. Lett. **122** 222001, DOI: `https://doi.org/10.1103/PhysRevLett.122.222001`.